

Article

An Integrated Cost-Aware Dual Monitoring Framework for SMPS Switching Device Diagnosis

Akeem Bayo Kareem , Ugochukwu Ejike Akpudo  and Jang-Wook Hur *

Department of Mechanical Engineering (Department of Aeronautics, Mechanical and Electronic Convergence Engineering), Kumoh National Institute of Technology, 61 Daehak-ro (Yangho-Dong), Gumi 39177, Gyeongbuk, Korea; 20216004@kumoh.ac.kr (A.B.K.); akpudougo@gmail.com (U.E.A.)

* Correspondence: hhjw88@kumoh.ac.kr

Abstract: The ability of a switch-mode AC/DC power supply to shrink supplies is a benefit and a requirement for most electronic devices with limited space. Major failures in switch-mode power supply (SMPS) during adverse working conditions are subject to mostly the switching devices and capacitors. For effective condition monitoring of the SMPS, dual (or multiple) sensing provides a more reliable standpoint against the traditional single sensing techniques as it provides a more comprehensive paradigm for accurate condition monitoring. This study proposes an integrated approach to SMPS condition monitoring by exploiting statistically extracted features from current and voltage signals for system fault diagnosis based on electrical stress. Following a correlation-based feature selection approach, salient features were utilized for improved fault detection and isolation (FDI) using ML-based classifiers. Diagnostic results by the classifiers reveal that the random forest and gradient boosting classifiers are highly reliable but computationally expensive when compared with the others while the decision tree was quite cost-efficient with reliable diagnostic results. The proposed framework is effectively applicable for use in diagnosing the switching devices and classification at different states.

Keywords: switched-mode power supply; switching devices; condition monitoring; machine learning; fault detection and isolation; dual monitoring



Citation: Kareem, A.B.; Ejike Akpudo, U.; Hur, J.-W. An Integrated Cost-Aware Dual Monitoring Framework for SMPS Switching Device Diagnosis. *Electronics* **2021**, *10*, 2487. <https://doi.org/10.3390/electronics10202487>

Academic Editors: Paolo Castaldi and Silvio Simani

Received: 12 September 2021

Accepted: 8 October 2021

Published: 13 October 2021

Publisher's Note: MDPI stays neutral with regard to jurisdictional claims in published maps and institutional affiliations.



Copyright: © 2021 by the authors. Licensee MDPI, Basel, Switzerland. This article is an open access article distributed under the terms and conditions of the Creative Commons Attribution (CC BY) license (<https://creativecommons.org/licenses/by/4.0/>).

1. Introduction

The past few decades have witnessed an uprising in technological advances and the emergence of industry 4.0, the reliability of industrial cyber-physical systems (ICPSs) becomes even more in demand [1]. While artificial intelligence (AI) remains the state-of-art alternative for most reliability solutions, predictive maintenance (PdM) becomes even more patronized than the traditional routine-based methods considering that recent solutions in the domain rely on the use of statistical principles on sensor data and AI-based methodologies for decision making [2].

Equipment/component condition monitoring under condition-based maintenance (CBM) schemes offers significant benefits ranging from reduced costs, uptime improvement, and downtime reduction. The availability of (and durability) of data-driven approaches to CBM has shown profound successes in recent times; yet, attaining a global paradigm for its use remains open for investigation, criticisms, improvements, and hopefully, generality [3]. On the bright side, recent studies [4,5] suggest that the use of multiple parameters (sensor measurements, features, etc.) for condition monitoring better provides a more reliable standpoint for diagnostic/FDI evaluations when compared with single parameters. Particularly for electronic components, because of their comparatively higher delicate nature (when compared with mechanical equipment/systems), the ability to predict failure at an early stage is crucial. In addition, ensuring their successful and long-term operation becomes even more crucial for increased profit, utility, and consumer satisfaction [6]. Con-

sequently, appropriately exploiting reflective parameters from these electronic components becomes necessary.

Power electronic devices are made up of separate components and modules that are subjected to thermal, chemical, electrical, and mechanical stressors, eventually leading to catastrophic failure. Various research has divided power electronics failure mechanisms into two categories: chip-related and packaged-related failures. Electrical over-stress, either by high voltage or high current, is the most popular trigger of chip failure, whereas thermal stress is the most common cause of packed device failure [7,8]. Numerous electrical parameters and ambient variables influence the operational characteristics of electronic components and devices, resulting in abrupt/uncertain failures before the intended lifetime, as indicated in the datasheet [9]. Particularly for electronic components, environmental factors affect their durability. For instance, according to [6], temperature changes has a 45% impact on the performance and longevity of electronic components, whereas vibration, humidity, dust, and stress all have a 20%, 19%, 6%, and 10% impact on the performance and longevity of electronic components respectively. Needless to say, uncertain factors also contribute marginally to most electronic component failures; hence the need for reliable multi-variable condition monitoring systems [1,2,4].

Electrical signature analysis (ESA) is one of the major techniques which is centered on the evaluation of the electrical signals of power electronics using signal processing methods for the discovery of, and evaluation of transient and spectral behaviors in the components. In this domain, current signature analysis (CSA), voltage signature analysis (VSA), and extended park's vector approach (EPVA) are quite popular and with appropriate methodologies, they can be integrated with an even more reliable ESA-based condition monitoring framework [10,11]. The idea and major intrigue ESA poses are in identifying faults in electrical systems by monitoring the frequency components during the healthy and faulty stage [12]. Feature and usage-based diagnostics and prognostics for electronic systems can be utilized by finding essential diagnostic parameters that coincide with failure progression and recognized failure models. To provide collective proof of a worsening or deteriorating condition, collected features can be identified, evaluated, and exploited for data-driven (AI-based) FDI [10,13,14]. From a realistic perspective, the complexity of electronic data, the vast number of parameters, conflicting failure mechanisms, and the prevalence of intermittent faults and failures make health management and assessment of electronic systems a difficult task. This makes it even more beneficial to exploit as many measurements (and features) as possible under a comprehensive framework to ensure that not only are optimal parameters are identified, but also, properly harnessed. This is especially true when working with complicated electrical systems, where different parameters (like the voltage, resistance, capacitance, etc.) reflect component conditions uniquely [15].

In this paper, we have been able to physically simulate loaded conditions for an SMPS device and proposed an integrated framework for condition monitoring. The proposed framework exploits statistical features from current and voltage signatures simultaneously and a machine learning model for FDI. Arguably, the efficiencies of time-frequency-domain feature extraction over the stand-alone time-domain or frequency-domain feature extraction methods are quite impressive; however, considering their relatively higher computational costs and peculiarity for vibration monitoring, the less computationally expensive technique—time-domain feature extraction provides a cost-efficient and reliable feature extraction method [4]. To achieve a more reliable diagnosis using these time-dependent signal processing methods, it is often wiser to explore as many features as possible to acquire a more diversified representation of the components. This provides an abundance of features to select from based on discriminance and salience using any (or a combination) of the numerous filter-based, wrapper-based, and/or hybrid feature selection methods available for exploration. Particularly for cost-aware systems, filter-based methods offer ease-of-use, high efficiency, fair reliability, and unbiasedness (considering that their functionality are

purely unsupervised). Furthermore, considering the integrated dual monitoring process (voltage and current), the rationale for cost efficiency becomes even more important.

The rest of the paper is structured thus: Section 2 presents the motivation for the study and relevant literature review while Section 3 summarizes the theoretical background of the constituent modules in the proposed study. Section 4 presents the proposed diagnostics framework while Section 5 presents the experimental validation of the proposed framework using ML-based classification algorithms (chosen based on experience-based knowledge and predictive capacity). Section 6 discusses the inherent experimental results and lastly, Section 7 presents a conclusion that helps to foster future research directions.

2. Motivation and Literature Overview

The working principle of a linear power supply denotes that for an output voltage to be achieved, the power circuits require a primary capacitor, a secondary capacitor, and more or fewer feedback resistors. Unlike the more common switched-mode power supplies (SMPS), which have replaced the classic linear-type AC with DC power supplies, reduced power consumption, heat dissipation, size, and lighter weight are some of the advantages of the switched-mode over the linear power supply. Most PCs, amplifiers, televisions, motor drives, and other electronic devices are presently set up with a power supply mechanism. More emphatically, the main advantage of an SMPS over a typical linear regulator is its better efficiency, which is obtained via a powerful internal switching device such as a transistor, power metal-oxide-semiconductor field-effect transistor (MOSFET), or Schottky diode.

Most often, a power supply like other sensitive electronic systems is designed to operate continuously, exposing it to a variety of failure mechanisms such as electrical stress, overuse/under-use, ambient conditions, and so on. As a result, real-time condition monitoring of the power supply is essential for accurate predictive maintenance. The switching transistor, whose role is to provide a high alternating voltage for the transformer, is one of the most critical risk-prone components following a failure mode effect analysis (FMEA) [16]. This hints at an increased need for ensuring that the SMPS operates under the recommended specifications to avoid unforeseen failure. On the brighter side, condition monitoring offers a cost-effective solution for controlled and uninterrupted functioning [14].

Several methods have been employed in the past for SMPS condition monitoring with reliable successes. Most traditional methods typically exploit the transient and/or spectral information in electrical signatures using domain knowledge guided by an understanding of the equipment's physics-of-failure (PoF) [17]. On the other hand, state-of-the-art methods exploit the efficiencies of AI techniques over PoF models especially for systems with a significant level of uncertainty. For instance, the wavelet-based analytical model developed in [18] for fault direction identification in relay agents uses the wavelet coefficient of measured line currents. Although the results validate the model's strengths through a simulation of a benchmark medium-voltage distribution system, the proposed analytical model lacks strong conviction for physical systems with significant uncertainty levels. In a different study [19], the authors proposed a fault diagnosis and reconfiguration method for 3-phase interleaved buck converters based on the output voltage for diagnosing open-circuit faults. The experimental evaluations on a hardware-in-the-loop test platform reveal high-speed computation efficiencies, ease-of-use, and high accuracy; however, the approach functions under ideal theoretical assumptions on VSA only. Another study took a different approach by exploring CSA methods. A hybrid grid system that contains a basic power supply was developed to achieve a fast switching fault diagnosis utilizing an instantaneous phase current [20].

Beyond ESA methods, other variables like temperature also provide reliable condition capabilities. In [8], a thermal approach was used to check for degradation of the semiconductors which was subjected to thermal aging. The major impression that inspires the author of this paper is the structure of the vigorous diagnostic that allows for a packaged

device of mostly electronics devices to be monitored under severe environmental conditions. In another study, as part of an incorporated methodology to power supply health management, a statistical consistency model, failure process analysis, enhanced aging, feature classification, sensor-based condition monitoring, and pattern recognition algorithms were given in [21]. Therein, the most common failure causes for SMPSs were found to be MOSFETs, IGBTs, and Schottky diodes with Time-dependent dielectric breakdown (TDDB) and the activation of parasitic structure using physics of failure analysis [22].

From a broader perspective, the authors believe that exploiting multiple parameters in a comprehensive framework would offer better reliable condition monitoring efficiencies since the efficiencies of one variable (VSA for instance) would complement the limitations of the other (CSA for instance). In this light, this study makes the following contributions:

- An integrated dual monitoring approach for SMPS switching devices is proposed. The model combines voltage and current signatures to achieve a more comprehensive condition monitoring framework for system fault diagnosis based on electrical stress.
- The proposed model considers cost-awareness by extracting statistical features from the electrical signals. Considering the computational costs associated with the most advanced signal processing techniques and the need for a dual feature extraction process (from current and voltage signals), the statistical feature extraction process offers a cost-efficient (yet highly reliable) alternative. The cost efficiency is further supported by a high-threshold correlation-based feature selection module for improved condition monitoring.
- Against the limitations of traditional analytical methods, the proposed model exploits the efficiencies of AI-based models for diagnosis. An exploratory comparison is presented between the employed ML-based classifiers and their performances assessed from different empirical standpoints.

3. Theoretical Review

3.1. AC–DC Switched Mode Power Supply

Ideally, an AC–DC SMPS converts AC power from the primary section to lower voltage DC power in the secondary section. Despite the fluctuations in the supply, it provides reliable DC output by regulating electric power. This is attributed to the voltage-controlled devices which form a major part of its functionality. Although diverse unique designs and configurations abound in the market, most SMPS devices are composed of an input electromagnetic interference filter (EMI), a rectification and filtering circuit, a power conversion circuit, a pulse width modulation (PWM) controller circuit, and an output rectification and filtering circuit [23]. Figure 1 illustrates a typical AC–DC SMPS configuration and the functional connections between/amongst them.

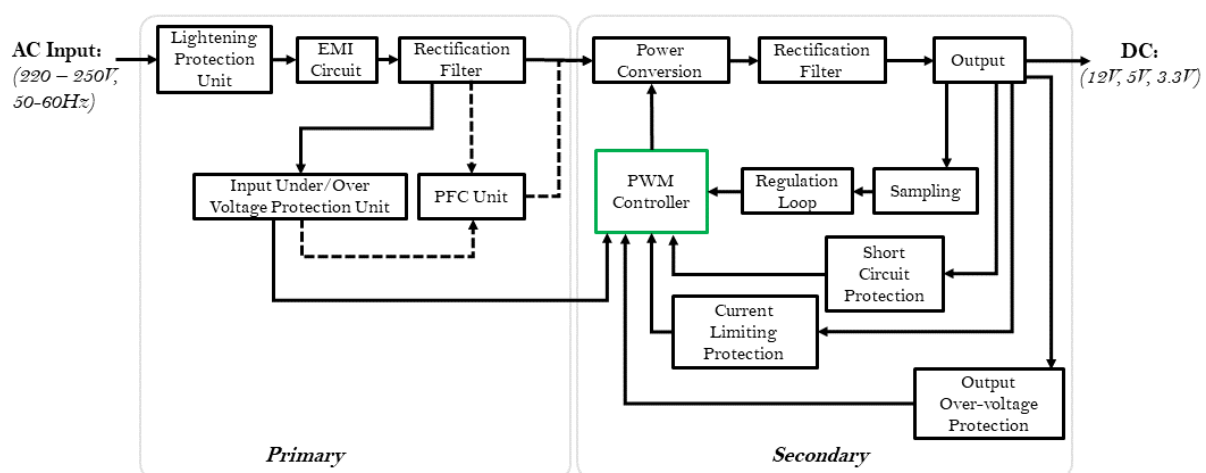


Figure 1. AC–DC Switched Mode Power Supply design.

As shown, the SMPS receives AC power (220–250 V, 50–60 Hz) at the EMI whose main function is to suppresses the electromagnetic noise and clutter signals of the input power source to prevent interference to the power supply. It also suppresses high-frequency clutter generated by the SMPS itself from interfering with the power grid. This is supported by the lightning protection unit (which consists of varistors) that impedes the increased voltage effect caused by lightning.

The rectification filter unit then rectifies (and filters) the AC voltage to obtain a relatively pure DC voltage with the aid of a capacitor. Next, the harmonic filter power factor correction (PFC) with the help of the input voltage protection unit provides automatic line-voltage adjustment, improves AC mains power quality in medium- and high-power applications, and stabilizes the SMPS bulk bus voltage. These features, in turn, improve cost factors and the holdup time of the isolated PWM converter. Presently, the most widely used power conversion device for SMPS devices is the MOSFET (MOS transistor) and is probably the most critical component of most SMPS devices [24]. As illustrated in Figure 2, the two different types of MOSFETs—P and N-type are illustrated. Overall, MOSFETs are voltage-controlled devices that function by utilizing the magnitude of the gate-source voltage (V_{GS}) to change the amount of induced charge on the semiconductor surface, thereby controlling the drain current (i_D) [25].

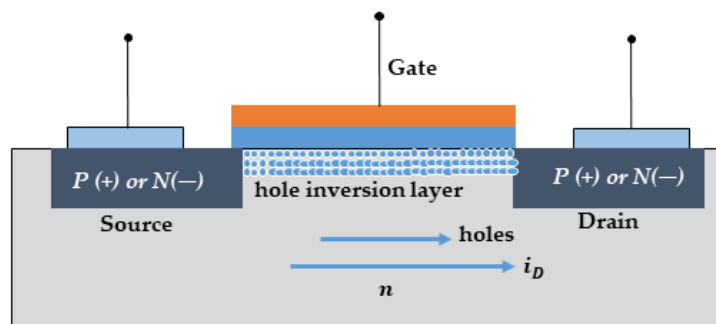


Figure 2. A typical P or N-channel MOSFET illustration.

Generally, the mode of operation of MOSFETs could either be a depletion type (P-channel) or enhancement type (N-channel) whereby enhancement types require the V_{GS} to switch the device “OFF” as is the case with a normally closed switch while the reverse is the case for a depletion type. When a negative gate voltage is applied (with a positive source voltage ($P+$)), the hole inversion layer is produced, allowing the current to flow to the drain to be turned on. On the other hand, when a positive gate voltage is applied (with a negative source voltage ($N-$)), the device is turned on. Ideally, the V_{GS} must be sufficient to drive the MOSFET into the ohmic zone and is expected to maintain a 12 V capacity. To provide a simpler illustration for understanding the modes of operation of the different types of MOSFETs, Table 1 provides the criteria/condition which the P-Channel and N-Channel turn ON and OFF.

Table 1. The switching characteristics for both N-channel and P-channel type MOSFETs.

MOSFET Type	$V_{GS} < 0$ (Negative)	$V_{GS} = 0$	$V_{GS} > 0$ (Positive)
N-channel Enhancement	OFF	OFF	ON
N-channel Depletion	OFF	ON	ON
P-channel Enhancement	ON	OFF	OFF
P-channel Depletion	ON	ON	OFF

The simplicity in design of P-Channel MOSFETs is beneficial for low-voltage drive compact board applications where space is limited. Its simplified gate driving technique often reduces overall cost and is more preferred over the N-Channel MOSFETs.

3.2. Electrical Signature Analysis

Electrical stress on electronics, in general, can induce component degradation or catastrophic failure during operation or handling. As a result of improper device application or use, electrical over-stress can occur, leading to parametric dilapidation or catastrophic failure; however, during the transfer test of exposed electronics, improper handling and a lack of effective electrostatic discharge (ESD) shielding may result in electrostatic discharge (ESD). These stresses are often reflected as electrical signals which when properly harnessed, can provide distinctive information for condition assessments.

Often, time-domain and frequency-domain signal processing techniques provide underlying features that can be linked to varying component conditions. The frequency-domain outputs—spectra (or electrical fingerprints) often present component conditions in a range of characteristic frequencies with different magnitudes which change as the component condition changes [26]; however, a major setback of this technique is that it functions on the assumption that the signals are stationary and requires a short period (a less than a second) of a signal for reliable analyses. These limitations render it less optimal for cases where fluctuations are witnessed in the electrical signals (high nonstationarity). In this case, exploiting time-domain statistical tools would provide superior efficiencies since they provide transient characteristics and are more cost-efficient. When certain faults occur, specific frequencies vary in magnitude. Fault patterns are frequency components that are elicited by each fault. They are largely determined by the machine's line frequency and structural parameters [13].

Arguably, time-frequency-domain signal processing techniques like a short-time Fourier transform (STFT), empirical mode decomposition (EMD), wavelet transform, mel frequency cepstral coefficients (MFCC), etc. offer superior efficiencies since they capture both transient and spectral characteristics; however, considering the high costs associated with them, their impact in the proposed study would only inhibit the cost awareness [13]. For instance, the EMD functions on the basis of the exhaustive iteration process, the STFT requires an optimal choice of window function which is often an uphill task, the wavelet transform depends on the optimal choice of matching wavelet while MFCC's efficiencies are preserved for low-frequency problems so maybe unfit for high-frequency fault detection or condition monitoring [4].

3.3. Review of ML Algorithms

AI has become predominant across most disciplines owing to its superiority over traditional statistical model-based approaches. In the domain, recent research trends suggest the use of the more robust deep learning (DL)-based methods artificial neural networks (ANNs) over the more fundamental machine learning (ML) algorithms like K-Nearest Neighbor(KNN), gradient boosting classifier (GBC) Support Vector Machines (SVM), Random Forest (RF), Decision Tree (DT), multi-layer perceptron (MLP), etc. Although characterized with superior detection and predictive accuracy, these ANNs are still faced with interpretability challenges, excessive parameters dependence, demands big data, over-fitting/under-fitting issues, computational cost, and complexity [2,13,27,28]. On the bright side, ML algorithms are more interpretable, easy to use, efficient with little data, resource-friendly, and reliable given the right inputs [2].

Numerous studies have proposed different improvements in these ML algorithms (and a hybrid combination of algorithms) with significant successes; however, each algorithm functions uniquely based on a set of pre-defined process rules. This makes their respective performance on a given set of inputs different, and with diverse parameter possibilities for each of them, achieving generality in their use still remains open for continued research. Notwithstanding, recent studies have observed some cost efficiency of these algorithms

under ideal conditions with some concurrent inferences which provide leeway for choosing amongst them. For instance, contrary to the RF algorithm and GBC, the KNN and DT are popularly known for computational cost-friendliness given the same set of inputs. The SVM and MLP are often disfavoured due to the strenuous parameter search associated with its use.

In reality, it would be futile to explore all these algorithms (and their different architectures and variants) in this study. Notwithstanding, experience in the domain and supporting research [4,29] RF, GBC, KNN, and SVM are quite robust for most classification problems and are employed in this study.

4. Proposed Diagnostic Framework

The descriptive procedure for the diagnostic approach is shown in Figure 3, whereby the model receives voltage and current signals from the data acquisition module. Overall, the proposed model consists of the following key modules—Two-way feature extraction, correlation-based feature selection, ML/DL-based diagnosis, and performance evaluation.

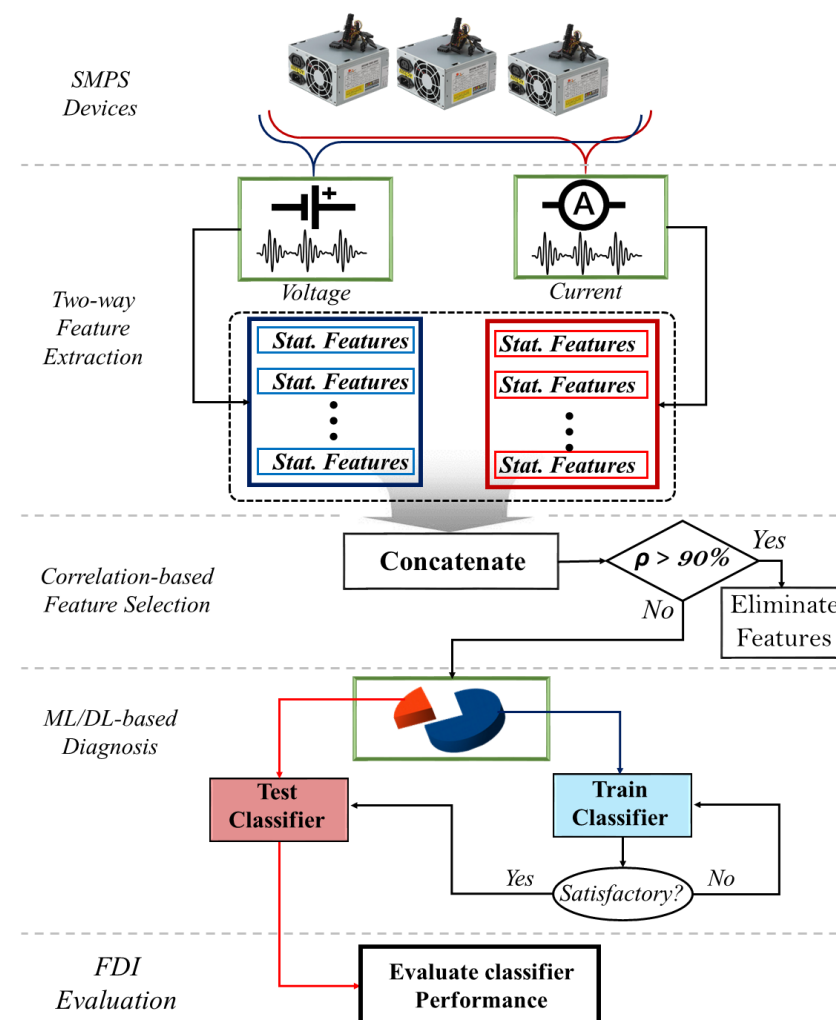


Figure 3. Proposed Framework for SMPS Switching Devices Model.

The voltage and current signals are simultaneously received by the model for a normalized feature extraction process. Particularly, the features summarized in Table 2 are extracted from the signals via a windowing approach—using a window size of 0.1 s (100 samples), the signals were split into equally spaced series, and on each of these portions, the features were extracted.

Table 2. Extracted Features and their definitions.

Feature Name	Definition
n th percentile ($n = 5, 25, 75, 95$)	$P_x = 100 \frac{x-0.5}{n}$
Root Mean Square	$X_{rms} = \sqrt{\frac{\sum_{i=1}^n (x_i)^2}{n}}$
Median	$\left(\frac{n+1}{2}\right)^{th}$ sample
Mean	$\bar{x} = \frac{1}{n} (\sum_{i=1}^n x_i)$
Kurtosis	$X_{kurt} = \frac{1}{N} \sum \left(\frac{(x_i - \mu)^3}{\sigma} \right)$
Interquartile range	$upperquarterQ_3 - lowerquarterQ_1$
Median abs deviation	$X_{mad} = \frac{1}{n} \sum_{i=1}^n x_i - m $
Standard error mean	$X_{sem} = \frac{standarddeviation}{\sqrt{n}}$
Geometric standard deviation	$X_{gstd} = \sqrt{\frac{\sum_{i=1}^N (x_i - \bar{x})^2}{n-1}}$
Skewness	$X_{skew} = E \left[\left(\frac{(x_i - \mu)^3}{\sigma} \right) \right]$
Max	$X_{max} = \max(x_i)$
Min	$X_{min} = \min(x_i)$
Crest Factor	$X_{CF} = \frac{x_{max}}{x_{rms}}$
Impulse Fcator	$X_{IF} = \frac{x_{max}}{\frac{1}{N} \sum_{i=1}^N x_i }$
Peak-to-peak	$X_{p-p} = x_{max} - x_{min}$
Peak factor	$x_{PF} = \frac{x_{max}}{\sqrt{x_s}}$
Wave Factor	$x_{WF} = \frac{\sqrt{\frac{1}{n} \sum_{i=1}^n x_i ^2}}{\frac{1}{n} \sum_{i=1}^n x_i }$
Clearance Factor	$x_{CF} = \frac{x_{max}}{\text{mean} 2x }$
Entropy	$x_E = - \sum_{i=1}^N P(x_i) \log P(x_i)$
Mean Crossing Rate	$x_{MCR} = \frac{\sum_{i=2}^n \sin(x_i - \mu) - \sin(x_{i-1} - \mu) }{2}$

It is common practice to capture as many features as possible [30]. This ensures that the underlying characteristics in the signals are well represented from diverse perspectives while also capturing the time-dependent information in the signals. By doing so, necessary transient evaluations may be conducted (if the need arises). Overall, the statistical feature extraction process presented herein was motivated by the cost awareness of the system owing to the potential costs associated with the two-way feature extraction if other advanced frequency-domain and/or time-frequency-domain signal processing methods were employed.

In addition to the above rationale, combining the extracted features from the current and voltage signals constitutes a high-dimensional feature space which also has some similarities amongst the extracted variables. Ideally, ML-based classifiers flourish based on the discriminance in the provided inputs. This presents an opportunity for feature selection after which, only discriminant features are retained, the curse of dimensionality is significantly minimized, computational costs are reduced, and the diagnostic/FDI performance is improved. Consequently, the correlation-based method of feature selection is employed for feature selection. This simple but effective statistical test which was developed by Karl Pearson in 1911 [31] is a measure for quantifying the linear dependence between two

variables X and Y and has a range of -1 (negative correlation) and $+1$ (positive correlation). This is obtained using Equation (1).

$$\rho_{X,Y} = \frac{\text{cov}(X,Y)}{\sigma_X \sigma_Y} \quad (1)$$

where σ_X and σ_Y are the standard deviations of X and Y , respectively while $\text{cov}(X,Y)$ is the covariance.

The selected features are then received by the ML classifiers for training and testing on the training and test datasets, respectively. The overall performance(s) is(are) finally evaluated.

5. Experimental Setup and Signal Processing

This section presents the methods that have been deployed to acquiring data from the accelerated life test setup to aid the machine learning-based classification approach for system fault diagnosis. Accelerated aging techniques open up a slew of possibilities for equipment condition monitoring and degradation assessments. They, for instance, make it possible to assess reliability in a fraction of the time it takes to undertake long-term reliability studies. Notwithstanding the time efficiency associated with the technique, it necessitates knowledge of the degradation process, quantities of critical productivity variables, and noticeable parameters in the augmented aging procedure.

As shown in Figure 4, the experimental setup consists of a DC load supply (PPL-8612c3, 150 V/60 A 300 W), the experimental case study—a 700 Watt SMSPS device (Hyper K Series/HP700S manufactured by FSP Group), and a NI 9174 DAQ device (affixed with NI 9221 and NI 9246 modules for acquiring voltage and current signals, respectively).

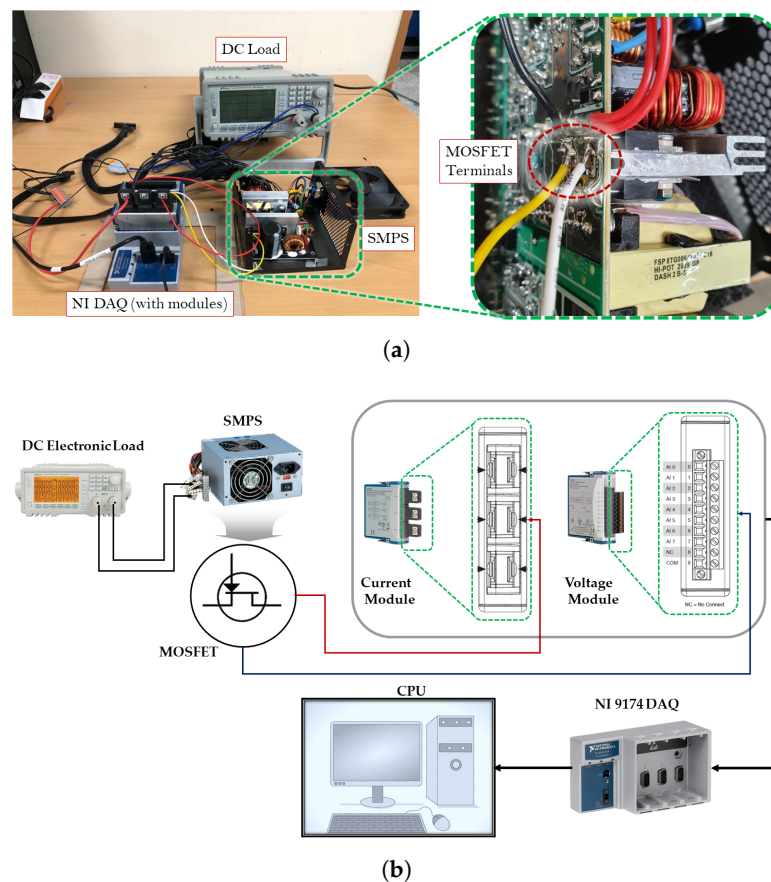


Figure 4. Experimental setup (a) a photo of the actual experimental setup, (b) an illustration of the data acquisition procedure.

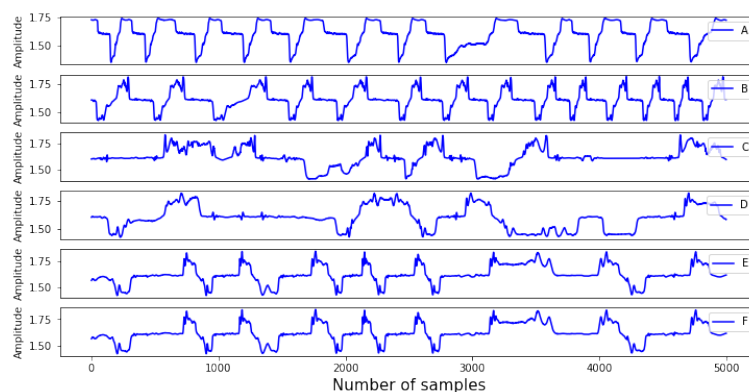
The DC load provides variable loading to the SMPS while the current and voltage signals are simultaneously acquired from the MOSFET terminals on the PCB. The cases study houses four (4) MOSFETS with a maximum root mean square voltage (V_{RMS}) of 31 V connected in parallel. Consequently, the current and voltage signals are then digitally collected from one of the MOSFET's terminals respectively by soldering two different pairs of wires to the terminals (each pair for the current and voltage signals respectively) while the other ends of the soldered wires are connected to the NI 9228 and NI 9246 modules respectively (see Figure 4). Digital data collection was done using a desktop computer with the aid of LabVIEW software at a sampling rate of 1KHz. The variable loading conditions are summarised in Table 3.

Table 3. The loading conditions for the experiment.

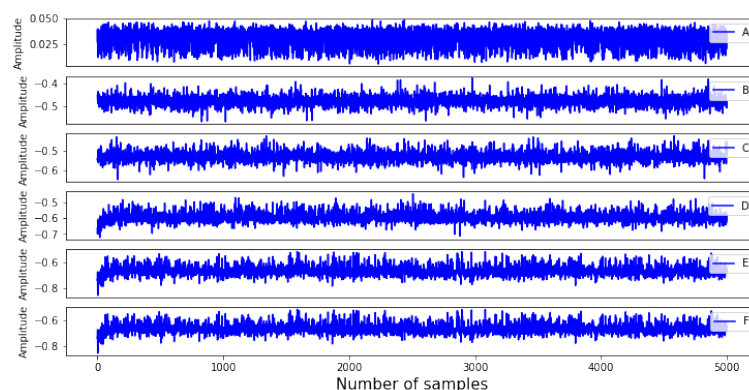
Cases (Label)	Electrical Loading (Watt)	Description
Case A (0)	0	No loading
Case B (1)	100	Small loading
Case C (2)	120	Fair loading
Case D (3)	140	Fairly high loading
Case E (4)	160	High loading
Case F (5)	170	Aggressive loading

5.1. Experimental Results

During the experiment, it was observed that the overall system's amperage increased as the loading increased; however, as Figure 5 shows, the impact of varying loading on the MOSFET could be observed directly from the raw signals as there are transient changes in the voltage and current signals, respectively.



(a)



(b)

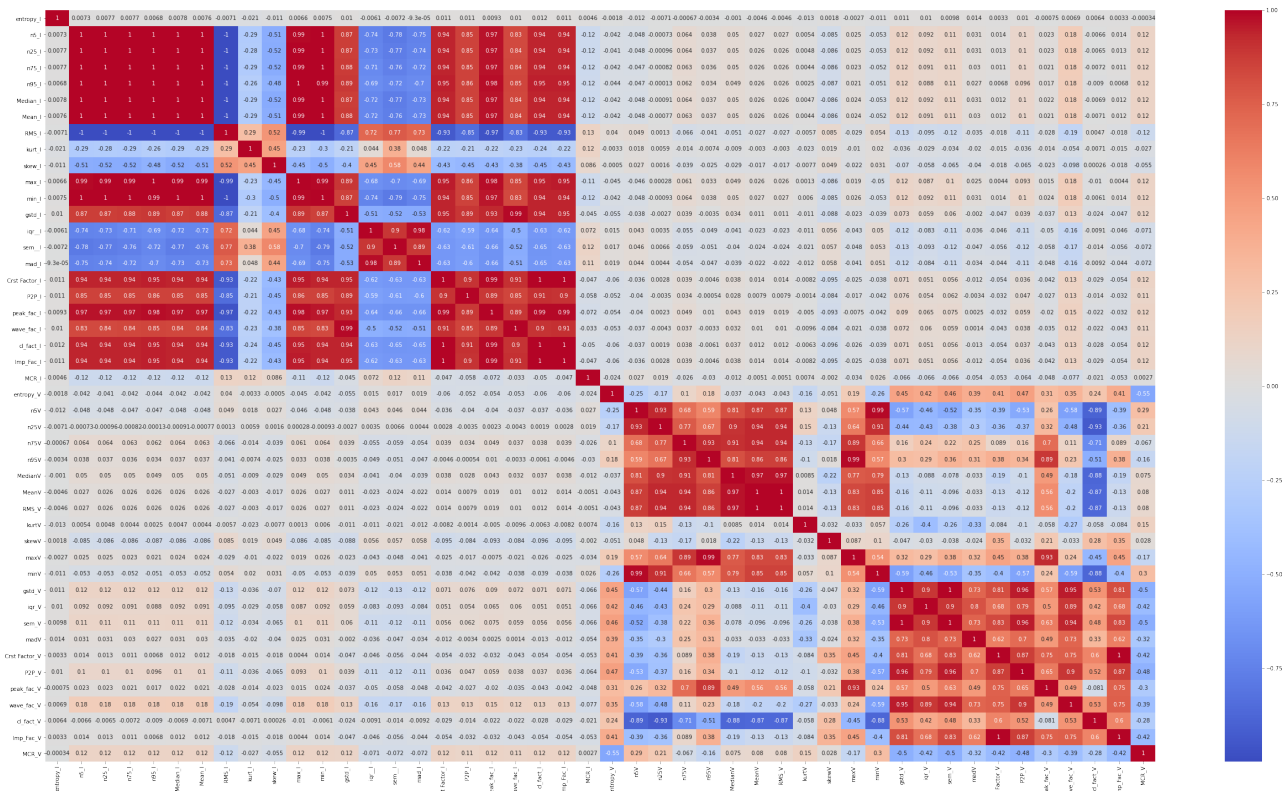
Figure 5. Experimental data at the various conditions (a) voltage signals. (b) current signals.

As shown in Figure 5a, at no loading condition (Case A), it is observed that a maximum voltage of ≈ 1.75 V is observed with periodic behavior. As loading is increased (Case A–F), new high-frequency components are observed; however, these high-frequency components have marginal relevance since the transient effect of the loading conditions are more reflected by the non-stationary behavior of the signals for the different conditions. This same assumption was considered for the current signals too since transient effects are also observed for the respective signals at the different conditions. Consequently, it would be more logical to exploit transient characteristics (features) for diagnosis.

5.2. Feature Engineering

Following the system model presented in Figure 6, the features summarised in Table 2 were extracted simultaneously from the voltage and current signals. An exhaustive observation of the extracted features revealed that each of the features (in their unique functionalities) were able to capture diverse transient information from the different signals; however, a correlation comparison would provide comparative assessments on their discriminance—the major selection criteria for diagnosis. Figure 6a shows the comprehensive correlation comparison of all the extracted features using Equation (1) while Figure 6b shows the selected features based on a 0.9 correlation threshold for selection.

As observed in Figure 6a, there are quite a number of highly correlated features (in red); however, upon implementing the feature selection, 21 features which include entropy, percentile, RMS, kurtosis, skewness, Geometric standard deviation, 5th percentile, interquartile range, crest factor, and mean crossing rate are highly discriminant in both current and voltage signals. On the other hand, features like peak-to-peak are uniquely discriminant in the current signals whereas features like clearance factor, median absolute deviation, and 75th percentile are uniquely discriminant in the voltage signals. Overall, the feature selection results reveal the comprehensive representation of the two-way features extraction process for SMPS condition monitoring.



(a)

Figure 6. Cont.

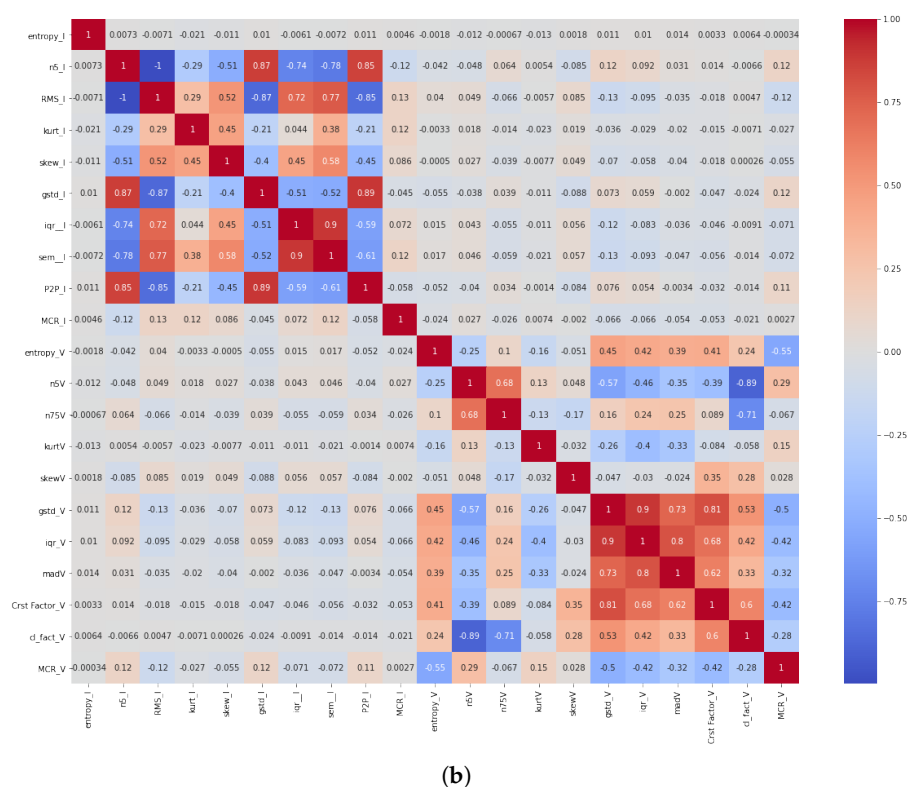


Figure 6. Correlation matrix of extracted features (a) All the features (b) 21 salient features.

6. Diagnostic Results and Assessments

6.1. Algorithm Initialization

Extracted condition indicators/features have a diverse set of interrelationships. Most classifiers would require features that are discriminant to reach respectable diagnostic accuracy. The feature selection results presented above are expected to provide acceptable diagnostic results and should serve as the right condition indicators for the SMPS. For ML-based diagnosis, the 21-dimensional selected features are extracted from the training data-set and test data-set respectively and prepared for training and evaluations.

Considering prior knowledge of the robustness and costs associated with ML-based classifiers, the algorithms presented in Table 4 were employed for diagnostic evaluation.

Table 4. ML classifiers and their respective parameters.

ML Classifier	Major Functional Parameters	Parameter Values
LR	Regularization	L1, L2
SVM Linear	gamma (γ)	γ = auto
SVM-RBF	Regularization (C), gamma (γ)	C = 100, γ = auto
KNN	k	18
DT	pruning	12
RF	n estimators	100
GBC	n estimators	100
MLP	Activation function (f), number of layers/nodes (h/a), learning rate (α)	f = ReLU, h/a = 1/7, α = 0.001
NBC	Gaussian	—

As shown above, each algorithm has its unique parameters and architecture and demands domain knowledge for optimum use. In reality, it would be futile to explore all the parameter possibilities for the respective algorithms; however, a grid search offers an av-

enue for discovering and the most befitting parameters for the respective algorithms. Consequently, the training process involved a grid search over a set of parameters, from which the validation set (20% of training data) is employed for training validation, after which testing is done using the test data set. To ensure an unbiased test evaluation, a 5-fold cross validation was done on each of the algorithms and the average score recorded.

6.2. Performance Evaluation Assessment

For test evaluation, standard classification evaluation metrics are employed. These metrics—accuracy, sensitivity/precision, recall, and F1-score provide a global assessment (as well as class-specific) on the classification performance of the models and are defined in Equations (2)–(5) [4]. In addition, the confusion matrix provides an avenue for closely assessing the class-specific predictions of the models for a more in-depth evaluation.

$$\text{Accuracy} = \frac{TP}{TP + FP + TN + FN} \quad (2)$$

$$\text{Sensitivity} = \frac{TP}{TP + FN} \quad (3)$$

$$\text{Precision} = \frac{TP}{TP + FP} \quad (4)$$

$$\text{F1-Score} = \frac{2 * \text{Sensitivity} * \text{Precision}}{\text{Precision} + \text{sensitivity}} \quad (5)$$

where the true positives (TP) are the number of accurately classified predictions, true negatives (TN) are the number of incorrectly labeled inputs belonging to correctly classified class, false positives (FP) are the number of incorrectly classified classes, and the false negatives (FN) are the number of incorrectly labeled inputs belonging to incorrectly classified class.

Another key factor to consider is the robustness of the algorithms and this can be assessed from the computational costs associated with each of the algorithms. Using the above-listed metrics, Table 5 summarizes the test performance of the models on the test data after 5-fold cross-validation as well as the average computational costs (in seconds) from the algorithms for one trial.

Table 5. Global performance comparison of ML models.

Algorithm	Accuracy (%)	Precision (%)	Recall (%)	F1-Score (%)	Cost (Secs)
LR	72.00	73.73	72.07	71.68	0.201176
SVM-Linear	96.37	96.33	96.35	96.33	0.873416
SVM-RBF	87.23	87.25	87.20	87.21	0.854272
k-NN	41.90	40.85	41.97	41.14	0.000610
DT	99.43	99.42	99.43	99.43	0.028453
RF	99.50	99.50	99.49	99.49	4.248675
GBC	99.50	99.51	99.49	99.50	66.616454
MLP	93.03	93.38	93.11	92.99	3.874173
NBC	98.77	98.83	98.72	98.75	0.002325

As observed from Table 5, the GBC and RF are the most accurate with accuracy, precision, recall, and F1-score of $\approx 99.5\%$ respectively; however, between the two, the GBC is the most computationally expensive with 66.6 s cost—about 16 times more expensive than the RF. The DT ranks next with a 99.43% accuracy but interestingly, it is one of the least expensive algorithms as shown by only a computational cost of 0.03 s (about 150 times faster than the RF). The NBC's and KNN's cost efficiency is observed by a 0.002 and 0.0006 s, respectively. Although the least expensive, the KNN's poor predictive performance as revealed by a 41.9% accuracy makes it unreliable for the proposed case study while the

DT offers a fairly acceptable performance with a test accuracy of 99.43%. Even with the exhaustive search for optimal k values for the KNN classifier as Figure 7 shows, its accuracy on the test data isn't encouraging.

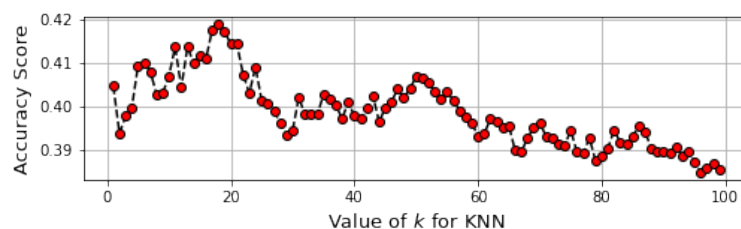


Figure 7. Test accuracy scores produced by the KNN model over different k values.

It can be observed the number of k neighbors suitable for the diagnosis process is at $k = 18$; however, even at this value, the test accuracy is $\approx 42\%$. Particularly for the SVM, the two variants—SVM-Linear and SVM-RBF were explored to assess the kernel efficiency between linear and nonlinear kernels. As observed, even at a fairly equal computational cost, the SVM-Linear outperforms the SVM-RBF by a difference of $\approx 9\%$ across the metrics—accuracy, precision, recall, and F1-score.

The presented evaluations offer a reliable rationale for choosing a classifier. In reality, computational speed often plays an important role in accepting/rejecting an algorithm. In this regard, the DT or NBC would suffice considering that although they are not the most accurate, they are more reliable with low costs and significant predictive accuracies. In contrast, the RF, MLP, and GBC would be considered for cost-unaware applications since they are the most accurate; yet the most expensive. In addition to the above results, the confusion matrix which provides a more class-specific evaluation of the classifiers' performance is presented in Figure 8.

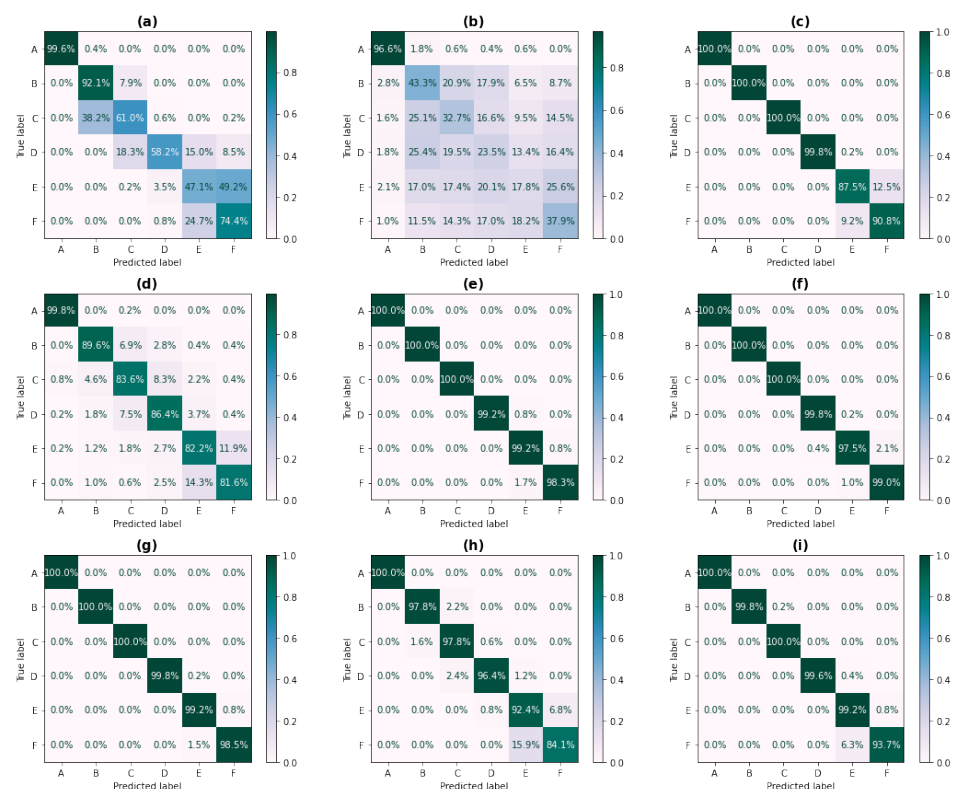


Figure 8. Confusion matrix by (a) LR, (b) SVM-Lin, (c) SVM-RBF ($C = 100$), (d) KNN, (e) DT, (f) RF, (g) GBC, (h) MLP, (i) NBC.

Overall, the confusion matrix results reveal that the FP, FN, TP, and TN (in percentage) for each prediction class by the respective classifiers. For instance, in Figure 8a, the LR's poor overall classification performance is observed from the low TP for the classes/labels (61% for C, 58.2% for D, 47.1% for E, and 74.4% for F). This is accompanied by significant FP and FN for each of the classes/labels. Also from Figure 8d, The KNN's poorest performance is observed from the class-specific FN and TN predictions for the classes/labels B–F. With such a poor performance, employing the KNN would invariably produce more false predictions. Contrary to the least accurate models, the other models' predictive accuracies are observed by the high TP for each class/label (between $\approx 81.6\%$ – 100%) across the whole algorithms. Interestingly, the RF's and GBC's high predictive accuracy are validated by the very low FP and FN values for each class (1.7% maximum).

7. Conclusions and Future Works

Likely one of the first attempts on a fault diagnostic approach of SMPS, this study proposed an ML-based diagnostics framework for SMPS by subjecting it to the electrical stress mode of failure. The SMPS has emerged as the cornerstone of efficient power transformation, converting mains voltage AC input to low voltage DC output. Analyzing the power supply switching operation which is a repeated on/off state which generates alternate current with high frequency at the primary side before being transferred through the transformer to the other side which is called the Secondary side. The voltage and current signals serve as the primary indicators of the switching device's degradation and condition of health in this investigation; however, necessary feature engineering further provides more reliable diagnostic parameters and were validated. An experimental test-bed was developed to monitor the switching device's behavior as it is subjected to external loading. Electrical signature analysis was used to analyze and visualize the behavior of the SMPS and switching devices under various electrical loading conditions using the various signal processing techniques. ML algorithms were used for fault diagnosis using uncorrelated statistical transient features from the current and voltage signals. The study aimed to find the best possible ML algorithm for the condition monitoring of the SMPS switching device with the RF and GBC being the most accurate and expensive while the DT was quite computationally efficient with high accuracy. In contrast, the KNN performed very poorly.

On the downside, the efficiency of the proposed diagnostic scheme will rely significantly on the operator/user experience since the feature selection threshold relies purely on user experience. This opens up room for human errors to creep in; however, it also opens up new opportunities for continued research. Considering the study explores only transient features (due to cost awareness), a cost-unaware application would require more advanced feature extraction techniques which would provide a more reliable avenue for improved trustworthiness and accuracy of the model. Ongoing research are aimed at exploring these solutions.

In future works, the authors intend to examine the SMPS using a temperature-dependent technique, by exposing the switching devices to temperatures outside of their permissible operating range for more precise condition monitoring. SMPS components in home items such as individual computers convert voltage and current features when transferring power from a DC or AC source to DC loads. SMPS are employed in all but the most rigorous uses to provide an efficient and effective source of power for most types of electronics systems as a result of their performance. Because of its relevance, having an accurate condition monitoring method that allows for an effective switching element maintenance strategy would be ideal.

Author Contributions: Conceptualization, A.B.K. and U.E.A.; methodology, A.B.K. and U.E.A.; software, A.B.K., U.E.A. and J.-W.H.; validation, U.E.A.; formal analysis, A.B.K. and U.E.A.; investigation, A.B.K. and U.E.A.; resources, J.-W.H.; data curation, A.B.K. and U.E.A.; writing—original draft preparation, A.B.K.; writing—review and editing, A.B.K. and U.E.A.; visualization, A.B.K. and

U.E.A.; supervision, J.W.H.; project administration, J.-W.H.; funding acquisition, J.-W.H. All authors have read and agreed to the published version of the manuscript.

Funding: This research was funded by MSIT(Ministry of Science and ICT), Korea, under the Grand Information Technology Research Center support program (IITP-2021-200-0-01612) supervised by the IITP(Institute for Information & communications Technology Planning & Evaluation).

Data Availability Statement: The data presented in this study are available on request from the corresponding author. The data are not publicly available due to laboratory regulations.

Conflicts of Interest: The authors declare no conflict of interest.

References

1. Yin, S.; Rodríguez-Andina, J.; Jiang, Y. Real-Time Monitoring and Control of Industrial Cyberphysical Systems: With Integrated Plant-Wide Monitoring and Control Framework. *IEEE Ind. Electron. Mag.* **2019**, *13*, 38–47. [\[CrossRef\]](#)
2. Akpudo, U.E.; Hur, J.W. Towards bearing failure prognostics: A practical comparison between data-driven methods for industrial applications. *J. Mech. Sci. Technol.* **2020**, *34*, 4161–4172. [\[CrossRef\]](#)
3. Ribeiro, M.T.; Singh, S.; Guestrin, C. Why Should I Trust You?: Explaining the Predictions of Any Classifier. *arXiv* **2016**, arXiv:1602.04938.
4. Akpudo, U.; Jang-Wook, H. A Multi-Domain Diagnostics Approach for Solenoid Pumps Based on Discriminative Features. *IEEE Access* **2020**, *8*, 175020–175034. [\[CrossRef\]](#)
5. Akpudo, U.E.; Hur, J. An Automated Sensor Fusion Approach for the RUL Prediction of Electromagnetic Pumps. *IEEE Access* **2021**, *9*, 38920–38933. [\[CrossRef\]](#)
6. Han, R.; Wang, R.; Zeng, G. Fault Diagnosis Method of Power Electronic Converter Based on Broad Learning. *Complexity* **2020**, *2020*, 7463291. [\[CrossRef\]](#)
7. Dong, G.; Miaohua, H. Prediction of Remaining Useful Life of Lithium-Ion Battery Based on Multi-Kernel Support Vector Machine with Particle Swarm Optimization. *J. Power Electron.* **2017**, *17*, 1288–1297. [\[CrossRef\]](#)
8. Ahmad, J.; Faiz, J.; Jarrahi, M.A. A Simple and Efficient Current Based Method for Inter-turn Fault Diagnosis of Brush-less Direct Current Motors. *IEEE Trans. Ind. Inform.* **2020**, *17*, 2707–2715. [\[CrossRef\]](#)
9. Kim, N.H.; An, D.; Choi, J.H. *Prognostics and Health Management of Engineering Systems: An Introduction*; Springer: Cham, Switzerland, 2017; pp. 127–241. [\[CrossRef\]](#)
10. Solanki, P.D.; Sharma, K.S. Determination of faults in 3- ϕ Induction Motor By Motor Current Signature Analysis. In Proceedings of the 2019 3rd International Conference on Recent Developments in Control, Automation & Power Engineering (RDCAPE), Noida, India, 10–11 October 2019; pp. 461–465. [\[CrossRef\]](#)
11. Balakrishna, P.; Khan, U. An Autonomous Electrical Signature Analysis-Based Method for Faults Monitoring in Industrial Motors. *IEEE Trans. Instrum. Meas.* **2021**, *70*, 3512008. [\[CrossRef\]](#)
12. Shifat, T.A.; Yasmin, S.R.; Hur, J.-W. A Data Driven RUL Estimation Framework of Electric Motor Using Deep Electrical Feature Learning from Current Harmonics and Apparent Power. *Energies* **2021**, *14*, 3156. [\[CrossRef\]](#)
13. Kim, S.; Akpudo, U.E.; Hur, J.-W. A Cost-Aware DNN-Based FDI Technology for Solenoid Pumps. *Electronics* **2021**, *10*, 2323. [\[CrossRef\]](#)
14. Shifat, T.A.; Hur, J. An Improved Stator Winding Short-circuit Fault Diagnosis using Adaboost algorithm. *Int. Conf. Artif. Intell. Inf. Commun.* **2020**, *2020*, 382–387. [\[CrossRef\]](#)
15. Shifat, T.A.; Hur, J. Motor Vibration Analysis for the Fault Diagnosis in Non-stationary Operating Conditions. *Int. J. Integr. Eng.* **2020**, *12*, 151–160. [\[CrossRef\]](#)
16. Rastayesh, S.; Rastayesh, B.; Sajjad, F.; Blaabjerg, F.; Zhou, D.; Zhou, W.; John, H.; John, S. A System Engineering Approach Using FMEA and Bayesian Network for Risk Analysis—A Case Study. *Sustainability* **2019**, *12*, 77. [\[CrossRef\]](#)
17. Sharma, P.K.; Bhargava, C.; Kotecha, K. Sustainability Analysis of a ZnO-NaCl-Based Capacitor Using Accelerated Life Testing and an Intelligent Modeling Approach. *Sustainability* **2021**, *13*, 10736. [\[CrossRef\]](#)
18. Nuwan, P.; Rajapakse, A.D.; Buchholzer, T.E. Isolation of faults in distribution networks with distributed generators. *IEEE Trans. Power Deliv.* **2008**, *23*, 2347–2355.
19. Li, P.; Li, X.; Zeng, T. A Fast and Simple Fault Diagnosis Method for Interleaved DC-DC Converters Based on Output Voltage Analysis. *Electronics* **2021**, *10*, 1451. [\[CrossRef\]](#)
20. Koo, G.W.; Joo, D.; Lee, B.K. Enhanced Threshold Point Calculation Algorithm for Switch Fault Diagnosis in Grid Connected 3-Phase AC-DC PWM Converters. *Energies* **2019**, *12*, 1979. [\[CrossRef\]](#)
21. Saufi, N.S.M.; Abdullah, N.S.Y.; Yaacob, M.I.H. LabVIEW-based data acquisition system for Diode I-V Characterization. *Adv. Sci. Technol. Eng. Syst. J.* **2018**, *3*, 348–351. [\[CrossRef\]](#)
22. Kou, L.; Liu, C. Fault diagnosis for power electronics converters based on deep feed forward network and wavelet compression. *Electr. Power Syst. Res.* **2020**, *185*, 106370. [\[CrossRef\]](#)
23. Galloway, K.F. A Brief Review of Heavy-Ion Radiation Degradation and Failure of Silicon UMOS Power Transistors. *Electronics* **2014**, *3*, 582–593. [\[CrossRef\]](#)

-
24. Rastayesh, S.; Bahrebar, S.; Bahman, A.S.; Sørensen, J.D.; Blaabjerg, F. Lifetime Estimation and Failure Risk Analysis in a Power Stage Used in Wind-Fuel Cell Hybrid Energy Systems. *Electronics* **2019**, *8*, 1412. [[CrossRef](#)]
 25. Nguyen, M.H.; Kwak, S. Enhance Reliability of Semiconductor Devices in Power Converters. *Electronics* **2020**, *9*, 2068. [[CrossRef](#)]
 26. Ismail, A.; Saidi, L.; Sayadi, M.; Benbouzid, M. A New Data-Driven Approach for Power IGBT Remaining Useful Life Estimation Based On Feature Reduction Technique and Neural Network. *Electronics* **2018**, *9*, 1571. [[CrossRef](#)]
 27. Akpudo, U.E.; Hur, J.-W. D-dCNN: A Novel Hybrid Deep Learning-Based Tool for Vibration-Based Diagnostics. *Energies* **2021**, *14*, 5286. [[CrossRef](#)]
 28. Akpudo, U.E.; Hur, J.-W. A CEEMDAN-Assisted Deep Learning Model for the RUL Estimation of Solenoid Pumps. *Electronics* **2021**, *10*, 2054. [[CrossRef](#)]
 29. Han, T.; Jiang, D.; Zhao, Q.; Wang, L.; Yin, K. Comparison of random forest, artificial neural networks and support vector machine for intelligent diagnosis of rotating machinery. *Trans. Inst. Meas. Control* **2018**, *40*, 2681–2693. [[CrossRef](#)]
 30. Shifat, T.A.; Hur, J.-W. ANN Assisted Multi Sensor Information Fusion for BLDC Motor Fault Diagnosis. *IEEE Access* **2021**, *9*, 9429–9441. [[CrossRef](#)]
 31. Galton, F. Co-relations and their measurement, chiefly from anthropometric data. *Proc. R. Soc.* **1888**, *45*, 135–145.